

# EFFECT OF ARC CURRENT ON MECHANICAL PROPERTIES OF AlCrN COATINGS DEPOSITED USING CATHODIC ARC EVAPORATION

*B. Warcholinski<sup>1</sup>, A. Gilewicz<sup>1</sup>, A.S. Kuprin<sup>2</sup>*

*<sup>1</sup>Koszalin University of Technology, Faculty of Mechanical Engineering, Koszalin, Poland;*

*<sup>2</sup>National Science Center "Kharkov Institute of Physics and Technology", Kharkiv, Ukraine*

*E-mail: bogdan.warcholinski@tu.koszalin.pl*

The AlCrN coatings were formed using cathodic arc evaporation at constant nitrogen pressure and arc current ranged from 50 to 120 A. Scanning electron microscopy, energy dispersive analysis, X-ray diffractometry, nanoindentation, adhesion tests and friction tests were used to investigate the effect of arc current on surface morphology, composition, structure, and mechanical and tribological properties of coatings. It was found that all coatings present cubic AlCrN with Al/(Al+Cr) ratio independent on arc current. Increase in the arc current results in increase in lattice parameter, crystallite size as well as deposition rate and coating surface roughness. A decrease in hardness with a simultaneous increase in Young's modulus is also observed. The adhesion of the coatings shows a non-linear character with the maximum (108 N) for the coating formed at an arc current of 80 A, which may explain the best wear resistance – the lowest wear rate  $1.4 \cdot 10^{-7} \text{ mm}^3/\text{Nm}$ .

PACS: 52.77.Dq, 52.80.Vp, 62.20.Qp, 81.10.Bk

## INTRODUCTION

Protective coatings applied to tools and machine parts increase their durability many times over. These coatings – nitrides, carbides, and borides of transition metals are characterized by good mechanical and tribological properties as well as good corrosion and oxidation resistance.

Such coatings are formed by Physical Vapor Deposition (PVD), including magnetron sputtering (MS), High-power impulse magnetron sputtering (HIPIMS), and cathodic arc evaporation (CAE), as well as Chemical Vapor Deposition (CVD).

The properties of the coatings depend not only on the method of their synthesis, but also on the technological parameters of the process: substrate temperature [1], reactive gas pressure [2, 3], substrate bias voltage [4, 5], but also the power during deposition (MS) or the arc current (CAE) [5, 6]. Due to the better mechanical properties of coatings formed by the CAE method compared to MS [7], the former method is used more often.

Due to high thermal resistance and hardness at high temperature, aluminum-doped CrN coatings are the subject of many studies and applications. These studies mainly cover the structure and phase composition [3, 4, 8], mechanical [3, 4, 6], and tribological [4, 6, 8] properties and thermal resistance [9]. It was found that the composition of the coatings [9] strongly influences their mechanical properties and microstructure. Another technological parameter that causes a similar nature of changes in coating properties is the substrate bias voltage [4, 8]. The reactive gas (nitrogen) pressure significantly changes the properties of the coatings [2, 3, 6]. With the increase in nitrogen pressure during coating formation, the phase transformation of  $\text{Cr} \rightarrow \text{Cr} + \text{Cr}_2\text{N} \rightarrow \text{Cr}_2\text{N} \rightarrow \text{Cr}_2\text{N} + \text{CrN} \rightarrow \text{CrN}$  is observed, as well as an increase in hardness and Young's modulus [2, 3], regardless of the method of coating formation, MS, and CAE. Another effect of the increase in nitrogen

pressure may be a change in the texture of the resulting coatings [3]. A similar effect is observed in coatings produced at different arc currents [5].

The improvement of the surface quality of the coatings formed by CAE can be obtained by adjusting the arc current [5]. Lowering the current can reduce the amount of macroparticles on the coating surface. However, a change in the arc current changes the plasma density. This may change the properties of the coatings. This effect has not been systematically tested for AlCrN coatings, and the presented results are inconclusive [5] compared to our preliminary studies. Lan et al. [5] found that with increasing arc current the grain size in the coating decreased from about 19 nm to about 11 nm and its hardness from about 2720 HV to about 2560 HV. This may be related to the reverse Hall-Petch effect. Our previous studies showed a similar size of crystallites (10...12 nm) in wide range of arc current and a slight increase in hardness with the arc current [6].

The aim of this paper is to check the influence arc current during deposition of AlCrN coatings from  $\text{Al}_{50}\text{Cr}_{50}$  cathode on their structure, morphology, mechanical, and tribological properties.

## MATERIALS AND EXPERIMENTAL TECHNIQUE

The ternary AlCrN coatings were formed by CAE method in semi-industrial TINA 900 M system (Vakuumtechnik Dresden GmbH, Germany). The 100 mm in diameter arc sources equipped with AlCr (50:50) alloy cathodes with 99.995% purity were applied. The substrates were: Si (30×3×0.52 mm) for stress measurements, 4H13 steel flat discs ( $\phi$  30 mm, 30 mm in thickness) for XRD analysis, HS6-5-2 steel flat discs ( $\phi$  32 mm, 3 mm in thickness) for mechanical investigations. Before deposition the steel substrates were ground and polished to roughness parameter Ra about 0.02  $\mu\text{m}$ . Then, to remove the organic contaminations they were ultrasonically cleaned in an

alkaline bath rinsed in deionized water and dried in warm air. After cleaning process the substrates were mounted on a rotating (about 2 rpm) holder within the vacuum chamber at a distance of 18 cm from the arc sources. The planetary type rotation was applied. After the chamber was evacuated to a pressure of  $10^{-3}$  Pa, ion etching of the substrate surface was performed with argon and chromium ions in an argon gas environment in order to remove surface oxides and improve the adhesion of the coatings to the substrate. Ion etching was conducted at argon pressure of 0.5 Pa, bias voltage of -600 V for 10 min, chrome cathode arc current 80 A. The substrate temperature during ion etching and coating deposition was about 350 °C. The second step to improve the adhesion of the coatings to the surface of the substrate was to apply a thin layer of chromium with a thickness of about 0.2  $\mu\text{m}$  directly to the cleaned substrate. The coatings were deposited using following parameters: substrate bias voltage of -100 V, nitrogen pressure of 4 Pa, and arc current ( $I_c$ ) in the range from 50 to 120 A. Considering the arc current ( $X$ ) during deposition, the designation of the coating is AlCr ( $X$ ) N. For example, AlCr(60)N denotes a coating formed at an arc current of 60 A.

The structure, thickness, surface morphology, mechanical properties, i.e. hardness, Young's modulus, stress and adhesion, and tribological properties, i.e. friction and wear were studied. The following methods and devices were used, see below:

1) coating thickness – Calotest – Spherical abrasion test method;

2) surface profile – contact profilometer, Hommel Tester T8000;

3) surface morphology and elemental composition – JEOL JSM-5500LV equipped with EDX, Oxford Link ISIS 300; optical microscope, Nikon Eclipse MA200;

4) phase composition – grazing incidence X-ray diffraction, Empyrean PANalytical. Cu-K $\alpha$  radiation (0.154056 nm) and the grazing incidence geometry at 3°. For data processing, HighScore Plus with ICDD PDF 4+ Database software (the Powder Diffraction File) was applied;

5) hardness – Fischerscope HM2000 hardness tester equipped with a Bercovich indenter. The average value of hardness and Young's modulus was calculated from at least 20 measurements;

6) adhesion – scratch tester (Revetest) equipped with diamond Rockwell C type indenter with 200  $\mu\text{m}$  radius. Scratch length was 10 mm, indenter speed – 10 mm/min, the average of at least three scratches. Critical loads:  $L_{c1}$  – the first coating failures appear, determined on the basis of the acoustic emission registered during the test and microscopic observations;  $L_{c2}$  – total delamination of the coating occur, determined from the microscopic observations.

Daimler-Benz test, it was performed by applying a force of 1471N to the coating. It is a qualitative destructive test for coating/substrate systems. In this method, damage to the layer adjacent to the Rockwell indentation boundary is observed and compared with a defined pattern of adhesion force.

7) friction and wear – ball on disc method. Counterpart: Al<sub>2</sub>O<sub>3</sub> ball, 10 mm in diameter, hardness of 15 GPa and Ra < 0.03  $\mu\text{m}$ . Test conditions: normal load 20 N, sliding speed 0.2 m/s, sliding distance of 2000 m, sliding radius – 12 mm, dry sliding ambient temperature, humidity around 50%.

Many details of the devices are in Ref. [6].

## EXPERIMENTAL RESULTS

In Fig. 1 are shown SEM images of surface morphology of AlCrN coatings formed at arc current of 50 A (see Fig. 1,a) and 120 A (see Fig. 1,b), i.e. the lowest and highest current of the arc source used in their formation. It is noticeable that as the arc current increases, the number of surface defects, macroparticles and craters also increases. At a higher arc current, more particles, also of larger sizes, are emitted from the cathode spot. The liquid cathode droplets deposited on the surface of the substrate solidify and form macroparticles. Thus, an increase in the arc current leads to a higher cathode energy and temperature and an increase in the number of emitted droplets from cathode material.

As shown in Fig. 1, the diameter of the macroparticles on both coatings formed at extreme arc currents is generally small, it does not exceed about 1.5  $\mu\text{m}$ , although there are macroparticles with a larger diameter. They are mostly oval in shape, however, irregularly shaped defects are also observed. A relatively large number of craters are also observed on the surface of the coatings, especially for AlCr(50)N. This may be due to the relatively low energy of the droplets hitting the surface, which means that they are easily removed by re-sputtering, leaving a blank space behind.

The roughness of the coatings depends on the development of the surface and depends not only on the type of its treatment (grinding, polishing, burnishing), but in the case of thin coatings also on the number of defects on its surface, i.e. macroparticles and craters. As already mentioned, as the arc current increases, the number of defects on the surface of the coatings increases. This variation in the surface quality of the coating is reflected in the roughness parameter Ra calculated as the average value of heights and depths on a given evaluation length. As shown in Table, an increase in the roughness parameter Ra from about 0.04  $\mu\text{m}$  (50 A) to about 0.12  $\mu\text{m}$  (120 A) is observed. The roughness parameter Rz as the difference between the tallest “peak” and the deepest “valley” on the evaluated length is about 10 times higher (see Table).

The recorded value of the roughness parameter Ra is much greater than for the substrate itself. The observed Ra value is similar to the results presented by other authors for aluminum-doped chromium nitrides or titanium nitrides [10, 11] applied by the method of cathodic arc vapor deposition. It should be noted that the CrN coatings obtained under the same conditions are characterized by lower roughness.

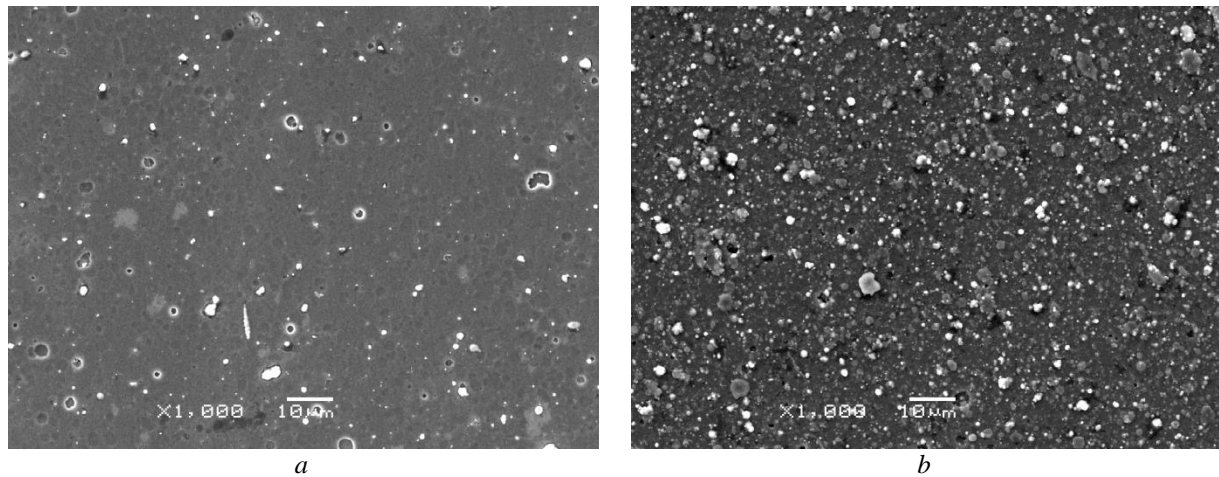


Fig. 1. SEM images of the AlCrN coating surfaces formed arc current: a – 50, b – 120 A

The results of the EDS tests of the elemental composition of the coatings are presented in Table. A small amount of oxygen in the coatings, decreasing with the current, as well as slight fluctuations in the concentrations of aluminum and chromium can be noticed. Their ratio for all coatings is similar and

amounts to about 0.45. This may be due to two reasons: different from the assumed cathode alloy composition, or higher scattering of Al atoms as a result of collisions with nitrogen and lower volume density in the vapor due to their lower atomic mass [12]. Such an effect for TiAlN coatings was confirmed earlier [13, 14].

Elemental composition, structural properties and mechanical characteristics of AlCrN coatings deposited at various arc current

Parameter		Arc current, A				
		50	60	80	100	120
Composition, at. %	Al	25.7	25.1	25	25.1	–
	Cr	31.3	31.6	31.2	30.5	–
	N	41.2	41.6	42.7	43.5	–
	O	1.9	1.7	1.1	0.9	–
Al/(Al + Cr)		0.451	0.443	0.445	0.451	–
(Al+Cr)/N		1.38	1.36	1.32	1.28	–
Lattice parameter, nm		0.4125	0.4131	0.4133	0.4134	0.4146
Crystallite size, nm		7.8	8.7	10.8	11.7	13.0
Deposition rate, nm/min		21.1	26.7	34.4	46.7	51.7
Roughness Ra, μm		0.04	0.05	0.06	0.071	0.12
Roughness Rz, μm		0.48±0.03	0.67±0.07	0.80±0.26	0.94±0.13	1.05±0.14
H, GPa		29.7±2.9	27.4±1.4	26.4±0.8	27.3±1.0	25.5±1.3
E, GPa		257±15	274±10	265±5	324±12	284±8
H/E		0.116±0.018	0.100±0.009	0.100±0.005	0.084±0.006	0.090±0.007
H <sup>3</sup> /E <sup>2</sup> , GPa		0.40±0.16	0.27±0.06	0.26±0.03	0.19±0.04	0.21±0.04
Stress, GPa		1.9	1.6	2.3	2.6	3.5
Critical load Lc <sub>2</sub> , N		71±6	93±1	108±1	85±1	77±4
CPRs, N <sup>2</sup>		1147±94	1656±204	1691±89	1520±132	1383±64
Wear rate, mm <sup>3</sup> /Nm		(7.1±0.3)·10 <sup>-7</sup>	(6.1±0.8)·10 <sup>-7</sup>	(1.4±0.7)·10 <sup>-7</sup>	(3.1±0.6)·10 <sup>-7</sup>	(4.8±1.0)·10 <sup>-7</sup>

Fig. 2 shows the XRD diffraction patterns of AlCrN coatings obtained with an arc current ranging from 50 to 120 A. It can be noticed that they have the same phase composition corresponding to the same elemental composition. The coatings are characterized by a cubic structure specific to CrN (ICDD card 04-004-6868). There are visible all diffraction lines in the range 30...120° corresponding to this phase; (111), (200), (220), (311), (222), (331), (420), and a line about 96° that is assigned to plane (400). The coatings are highly

textured. The most intense diffraction lines come from the planes (111) and (200). The plane (111) in the CrN structure is more densely packed than the plane (200). This may be the reason for the smoother coating surface with the dominant line (111). Such oriented coatings should show high density and adhesion to the substrate [11]. The ratio (200)/(111) of the line intensity for the coating produced at 50 A arc current is 2.29 and decreases to 0.42 (I<sub>c</sub> = 120 A).

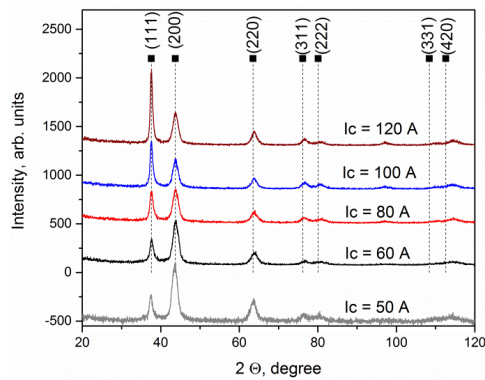


Fig. 2. X-ray diffraction patterns of AlCrN coatings with different arc currents

Farkas et al. [15] observed that the ZrN coatings produced by magnetron sputtering are characterized by a different ratio of the (200)/(111) line intensity. It decreases with increasing nitrogen pressure. He also observed a similar change for the roughness of the coatings. A similar nature of the changes in the intensity of the diffraction lines can be seen in the presented studies (see Fig. 2). However, the results of the roughness tests (see Table), do not confirm the above conclusions. It seems that this may be related to a different coating formation technology and its basic disadvantage – a large amount of macroparticles on the surface, which worsens its quality.

No diffraction lines from the substrate, the adhesive layer (Cr) or other chromium or aluminum phases: Cr<sub>2</sub>N, AlN were observed in the coatings.

The increase in the arc current leads to a slight increase in the lattice parameter from 0.4125 nm (Ic = 50 A) to 0.4146 nm (Ic = 120 A), which results from the shift of the diffraction lines towards lower angles. Simultaneously, the crystallite sizes were calculated (see Table). They increase from about 8 nm to about 13 nm at the extreme arc currents during the coating formation. It confirms our previous investigations [6], and is in opposite to results presented by Lan et al. [5], where with increase in arc current the crystallite size decreases.

Cubic CrN (ICDD card 04-004-6868) and AlN (ICDD card 04-012-3388) phases are characterized by the same space group Fm-3m (space group number 225) and lattice constant 0.4145 and 0.4052 nm, respectively. The diffraction lines from these phases are slightly shifted, about 0.9 for the (111) plane. The similar crystal structure of the above phases allows the formation of a cubic Al-Cr-N solid solution. The metal atoms are located at the sites of the fcc lattice, while the nitrogen atoms occupy the octahedral voids of the base metal.

The basic mechanical characteristics of the obtained coatings: hardness H, Young's modulus E, stress are summarized in Table. It can be noticed that with the increase of the arc current, the hardness gradually decreases and the Young's modulus increases slightly. A similar effect is shown in Ref. [5].

The reduction in hardness may be due to an increase in the size of the crystallites, although the increase in stress in the coatings with increasing arc current (see Table) should contribute to the increase in the hardness of the coatings. Due to relatively high substrate bias

voltage (-100 V) ion bombardment of the coating results in its higher compactness. Similar effect present the higher arc current. As a result of such interaction, the stress in the coating increases, as shown in Table. However, a secondary effect of high energy ion bombardment is an increase in substrate temperature. This can result in crystallite growth, as demonstrated previously. An additional effect is an increase in the amount of macroparticles and a greater amount of voids, which contributes to a reduction in hardness. All the above-mentioned mechanisms causing the increase and reduction of hardness compete with each other during the formation of the coating. The reduction in hardness, observed here, suggests that the increase in surface defects may be more important than the increase in coating density.

A similar effect, i.e. an increase in coating roughness, Young's modulus and compressive stresses with an increase in TiN thickness synthesized by the arc ion plating method, is presented in Ref. [16].

The assessment of the adhesion of coatings to the substrate was carried out using two tests: the scratch test, in which can be obtained the numerical value of the so-called the critical load L<sub>c</sub>, at which delamination occurs, and the Daimler-Benz test, in which the types of damage of the coating as a result of forcing a Rockwell C indenter into it with a force of about 1500 N are described. The latter method makes it possible to qualitatively assess the damage to the coating.

The scratch test results show a non-linear dependence of the critical load L<sub>c2</sub> with the current (see Table). L<sub>c2</sub> grows from about 71 N (Ic = 50 A) to about 108 N (Ic = 80 A), and then decreases to about 77 N (Ic = 120A). The above values are very high and indicate good adhesion of the coatings to the substrate.

The above adhesion results were confirmed in the Daimler-Benz test. Under load, the steel substrate deforms and there are only slight radial cracks, which, in the absence of delamination of the coating, indicate increased cohesion and adhesion of the coatings. Fig. 3 shows the micrograph of deformation for the coating characterized by the lowest critical force of all the tested, formed at Ic = 120 A. Only circumferential cracks can be noticed, probably related to the generation of high tensile stresses. Such stresses may be caused by piling up of the substrate material around a indentation in the D-B test. This effect occurs mainly in hard and brittle coatings [17].

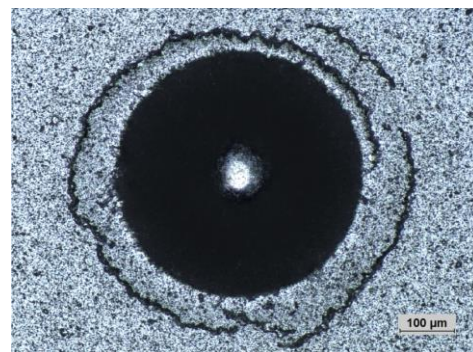


Fig. 3. The micrograph of Rockwell-C indents in AlCrN coating formed at arc current Ic = 120 A after the Daimler-Benz test

Despite the stresses occurring, no typical chips or coating delamination was observed at the boundary of the indentation. The observed damage to the coating does not reduce its functional properties. The large difference between the  $L_{c1}$  and  $L_{c2}$  loads indicates the wear resistance of the coating.

As mentioned previously, the critical force  $L_{c1}$  indicates the first failure of the coating and is therefore an indicator of the crack initiation resistance. With a high  $L_{c1}$ , thin coatings should show good adhesion. Zhang et al. [18] showed that both high  $L_{c1}$  and difference ( $L_{c2} - L_{c1}$ ) are required for high coating toughness. They presented a new parameter, called Scratch Crack Propagation Resistance ( $CPR_s$ ), as a  $CPR_s = L_{c1} (L_{c2} - L_{c1})$ . It is quick qualitative indicator of film toughness. It was found that  $CPR_s$  have a shape similar to the inverted parabola, with the maximum for AlCr(80)N coating (see Table).

In the analysis of coating wear processes the inverse relationship, the parabola with the minimum wear rate for AlCr(80)N coating, was observed (see Table). There is therefore a relationship between  $CPR_s$  and the wear rate: the higher the  $CPR_s$ , the greater the wear resistance.

The wear-resistant coating is characterized by a set of unique properties: high hardness, good adhesion and ductility. Transition metal nitride coatings are mostly characterized by high hardness, as well as various values of the elastic modulus  $E$ . According to many authors, the hardness and Young's modulus from the indentation test enable to predict the wear of coatings [19]. The  $H/E$  ratio is commonly used to describe the coating durability (the elastic strain to failure) [19]. It is assumed that the  $H/E$  value of 0.1 separates two zones: elastic ( $H/E > 0.1$ ) and plastic zone ( $H/E < 0.1$ ) [20]. Coatings with a higher  $H/E$  value should have a higher wear resistance. The  $H^3/E^2$  ratio may characterize the resistance to plastic deformation [21]. An almost linear decrease (with the arc current) in the  $H/E$  value from about 0.12 to about 0.09 is observed. The same trend occurs for the  $H^3/E^2$  index, an almost linear decrease from about 0.40 ( $I_c = 50$  A) to about 0.20 ( $I_c = 120$  A) (see Table).

This suggests that the coatings formed at 50 and 60 A should have better wear resistance. There is a discrepancy between  $CPR_s$ ,  $H/E$  and  $H^3/E^2$  indexes. However, it is worth noting the high value of the measurement uncertainty for these coatings. As a result, the lower value of the measuring range for individual coatings (after subtracting the measurement uncertainty) is similar in nature to the  $CPR_s$  trend. The highest wear resistance of coatings should be for the coating formed at arc current of 80 A, which is confirmed by the data of the wear process (see Table).

The above results are in line with the findings of Beake et al. [22].

## CONCLUSIONS

The paper presents the results and their analysis for coatings formed using the CAE at arc currents from 50 to 120 A. The research covered the structure, chemical and phase composition of the coatings, its mechanical

properties – hardness, Young's modulus, stress, adhesion, and tribological – friction and wear.

It was found that all coatings are characterized by the cubic structure B1, with an increasing (with arc current) value of the lattice parameter. The size of crystallites shows a similar dependence. The Al/(Al+Cr) ratio is approximately constant at about 0.45, which is less than the composition of the AlCr cathode used (50:50). This may be due to a different cathode chemical composition than desired or to greater scattering of Al atoms as a result of a collision with nitrogen. As the arc current increases, the ratio (Al+Cr)/N decreases. As expected, both the coating deposition rate and the surface roughness increase with the arc current. Roughness is the result of more macroparticles on the surface, mostly not exceeding 1.5  $\mu\text{m}$ .

Hardness generally decreases with arc current, while Young's modulus increases, which causes both  $H/E$  and  $H^3/E^2$  to decrease. The adhesion of the coatings determined by the scratch test is high, above 70 N, and it reaches the maximum (108 N) for a coating formed at an arc current of 80 A. The lowest value of the wear rate ( $1.4 \cdot 10^{-7}$   $\text{mm}^3/\text{Nm}$ ) is achieved by the same coating. The  $CPR_s$  index, the toughness of the coating, also confirms the observed character of the wear resistance of the coatings.

## ACKNOWLEDGEMENT

Publication partly financed by the National Centre for Research and Development, Poland, BIOSTRATEG3/344303/14/NCBR/2018.

## REFERENCES

1. B. Warcholinski, A. Gilewicz, P. Myslinski, E. Dobruchowska, D. Murzynski. Structure and Properties of AlCrN Coatings Deposited Using Cathodic Arc Evaporation // *Coatings*. 2020, v. 10, N 793, 21 p.
2. J.F. Tang, C.Y. Lin, F.C. Yang, C.L. Chang. Influence of Nitrogen Content and Bias Voltage on Residual Stress and the Tribological and Mechanical Properties of CrAlN Films // *Coatings*. 2020, v. 10, N 546, 13 p.
3. L. Wang, S. Zhang, Z. Chen, J. Li, M. Li. Influence of deposition parameters on hard Cr–Al–N coatings deposited by multi-arc ion plating // *Applied Surface Science*. 2012, v. 258, p. 3629-3636.
4. J. Romero, M.A. Gómez, J. Esteve, F. Montalà, L. Carreras, M. Grifol, A. Lousa. CrAlN coatings deposited by cathodic arc evaporation at different substrate bias // *Thin Solid Films*. 2006, v. 515, p. 113-117.
5. R. Lan, C. Wang, Z. Ma, G. Lu, P. Wang, J. Han. Effects of arc current and bias voltage on properties of AlCrN coatings by arc ion plating with large target // *Materials Research Express*. 2019, N 6, p. 116457 (9 p.).
6. A. Gilewicz, T. Kuznetsova, S. Aizikovich, V. Lapitskaya, A. Khabarava, A. Nikolaev, B. Warcholinski. Comparative Investigations of AlCrN Coatings Formed by Cathodic Arc Evaporation under

Different Nitrogen Pressure or Arc Current // *Materials* 2021, v. 14(2), N 304, 20 p.

7. G.G. Fuentes, R. Rodriguez, J.C. Avelar-Batista, J. Housden, F. Montal'a, L.J. Carreras, A.B. Cristobal, J.J. Damborenea, T.J. Tate. Recent advances in the chromium nitride PVD process for forming and machining surface protection // *Journal of Materials Processing Technology*. 2005, N 167, p. 415-421.

8. J.L. Mo, M.H. Zhu. Sliding tribological behavior of AlCrN coating. // *Tribology International*. 2008, v. 41, p. 1161-1168.

9. A.E. Reiter, V.H. Derflinger, B. Hanselmann, T. Bachmann, B. Sartory. Investigation of the properties of Al<sub>1-x</sub>Cr<sub>x</sub>N coatings prepared by cathodic arc evaporation // *Surface and Coatings Technology*. 2005, v. 200, p. 2114-2122.

10. A.E. Reiter, C. Mitterer, M.R. de Figueiredo, R. Franz. Abrasive and adhesive wear behavior of arc-evaporated Al<sub>1-x</sub>Cr<sub>x</sub>N hard coatings // *Tribology Letters*. 2010, v. 37, p. 605-611.

11. F. Cai, S. Zhang, J. Li, Z. Chen, M. Li, L. Wang. Effect of nitrogen partial pressure on Al-Ti-N films deposited by arc ion plating // *Applied Surface Science*. 2011, v. 258, p. 1819-1825.

12. Y.Y. Chang, D.Y. Wang, C.Y. Hung. Structural and mechanical properties of nanolayered TiAlN/CrN coatings synthesized by a cathodic arc deposition process // *Surface and Coatings Technology*. 2005, v. 200, p. 1702-1708.

13. H. Ohnuma, N. Nihira, A. Mitsuo, K. Toyoda, K. Kubota, T. Aizawa. Effect of aluminium concentration on friction and wear properties of titanium aluminium nitride films // *Surface and Coatings Technology*. 2004, v. 177-178, p. 623-626.

14. Y.Y. Chang, S.J. Yang, D.Y. Wang. Structural and mechanical properties of TiAlN/CrN coatings synthesized by a cathodic-arc deposition process // *Surface and Coatings Technology*. 2006, v. 201, p. 4209-4214.

15. N. Farkas, G. Zhang, R.D. Ramsier, E.A. Evans, J.A. Dagata. Characterization of Zirconium Nitride Films Sputter Deposited 609 with an Extensive Range of Nitrogen Flow Rates // *Journal of Vacuum Science Technology A*. 2008, v. 26(2), p. 297-301.

16. D.A. Colombo, M.D. Echeverría, R.C. Dommarco, J.M. Massone. Influence of TiN coating thickness on the rolling contact fatigue resistance of austempered ductile iron // *Wear*. 2016, v. 350-351, p. 82-88.

17. C. Rebolz, H. Ziegele, A. Leyland, A. Matthews. Structure, mechanical and tribological properties of nitrogen-containing chromium coatings prepared by reactive magnetron sputtering // *Surface and Coatings Technology*. 1999, v. 115, p. 222-229.

18. S. Zhang, D. Sun, Y. Fu, H. Du. Effect of sputtering target power on microstructure and mechanical properties of nanocomposite nc-TiN/a-SiN thin films // *Thin Solid Films*. 2004, v. 447-448, p. 462-467.

19. A. Leyland, A. Matthews. On the significance of the H/E ratio in wear control: a nanocomposite coating approach to optimised tribological behaviour // *Wear*. 2000, v. 246, p. 1-11.

20. A. Pogrebnyak, V. Beresnev, O. Bondar, B. Postolnyi, K. Zaleski, E. Coy, S. Jurga, M. Lisovenko, P. Konarski, L. Rebuta, J.P. Araujo. Superhard CrN/MoN coatings with multilayer architecture // *Materials Design*. 2018, v. 153, p. 47-59.

21. J. Musil, F. Kunc, H. Zeman, H. Polakova. Relationships between hardness, Young's modulus and elastic recovery in hard nanocomposite coatings // *Surface and Coatings Technology*. 2002, v. 154, p. 304-313.

22. B.D. Beake. The influence of the H/E ratio on wear resistance of coating systems – Insights from small-scale testing // *Surface and Coatings Technology*. 2022, v. 442, p. 128272.

Article received 15.08.2022

## ВПЛИВ СТРУМУ ДУГИ НА МЕХАНІЧНІ ВЛАСТИВОСТІ ПОКРИТТІВ AlCrN, ОСАДЖЕНИХ ЗА ДОПОМОГОЮ КАТОДНО-ДУГОВОГО ВИПАРОВУВАННЯ

Б. Вархолінський, А. Гілевич, О.С. Купрін

Покриття AlCrN були осаджені за допомогою катодного дугового випаровування при постійному тиску азоту та струмі дуги в діапазоні від 50 до 120 А. Використовували скануючу електронну мікроскопію, енергодисперсійний аналіз, рентгенівську дифрактометрію, наноіндентування, тести на адгезію та на тертя для дослідження ефекту впливу струму дуги на морфологію поверхні, склад, структуру, механічні та трибологічні властивості покриттів. Було виявлено, що всі покриття містять кубічний AlCrN із співвідношенням Al/(Al+Cr), не залежним від струму дуги. Збільшення струму дуги призводить до збільшення параметра решітки, розміру кристалітів, а також швидкості осадження та шорсткості поверхні покриття. Також спостерігається зниження твердості з одночасним збільшенням модуля Юнга. Адгезія покриттів має нелінійний характер з максимумом (108 Н) для покриття, сформованого при струмі дуги 80 А, що може пояснити найкращу зносостійкість – найменша швидкість зношування  $1,4 \cdot 10^{-7}$  мм<sup>3</sup>/Нм.